Experimental Eye Research 199 (2020) 108196

Contents lists available at ScienceDirect

Experimental Eye Research

journal homepage: www.elsevier.com/locate/yexer

Research article

A pathoconnectome of early neurodegeneration: Network changes in retinal degeneration

Rebecca L. Pfeiffer [a,*], James R. Anderson [a], Jeebika Dahal [a], Jessica C. Garcia [a], Jia-Hui Yang [a], Crystal L. Sigulinsky [a], Kevin Rapp [a], Daniel P. Emrich [a], Carl B. Watt [a], Hope AB Johnstun [a], Alexis R. Houser [a], Robert E. Marc [a,b], Bryan W. Jones [a,**]

[a] John Moran Eye Center at the University of Utah, Salt Lake City, UT, USA
[b] Signature Immunologics, Torrey, UT, USA

ARTICLE INFO

Keywords:
Connectomics
Pathoconnectomics
Retinal degeneration
Retinitis pigmentosa
Neurodegeneration
Abnormal ribbon morphology
Rod pathway
GABAergic amacrine cells

ABSTRACT

Connectomics has demonstrated that synaptic networks and their topologies are precise and directly correlate with physiology and behavior. The next extension of connectomics is pathoconnectomics: to map neural network synaptology and circuit topologies corrupted by neurological disease in order to identify robust targets for therapeutics. In this report, we characterize a pathoconnectome of early retinal degeneration. This pathoconnectome was generated using serial section transmission electron microscopy to achieve an ultrastructural connectome with 2.18nm/px resolution for accurate identification of all chemical and gap junctional synapses. We observe aberrant connectivity in the rod-network pathway and novel synaptic connections deriving from neurite sprouting. These observations reveal principles of neuron responses to the loss of network components and can be extended to other neurodegenerative diseases.

1. Introduction

1.1. Connectomics

The precise organization of neurons and their connections in brain, retina, and spinal cord defines network topologies underlying healthy nervous system processing (Marc et al., 2013). This has been demonstrated in numerous neural networks from spinal circuits (Catela et al., 2015), to *C. Elegans* (White et al., 1986), to the cerebral cortex (Lee et al., 2016), where distinct classes of neurons participate in synaptic networks to create precise network topologies. The study of all of the synaptic connections (ideally both chemical and electric) between all cells in a given neural network is termed *connectomics*. In 2011, we published the first retinal connectome, *Retinal Connectome 1* (RC1): an ultrastructural connectome of rabbit retina generated to elucidate the neural networks in retina contributing to visual processing (Anderson et al., 2011a). Many papers have detailed the specificity of retinal network motifs (Diamond, 2017; Thoreson and Dacey, 2019; Thoreson and Witkovsky, 1999; Tsukamoto and Omi, 2015, 2014, 2013), including those deriving from RC1 (Anderson et al., 2011a; Lauritzen et al., 2013; Lauritzen et al., 2019; Marc et al., 2014; Marc et al., 2018; Sigulinsky et al., 2020), but there are many more motifs yet to discover, particularly those involving inhibitory networks and glial interactions (Pfeiffer et al., 2019).

1.2. Why the retina

The retina is an ideal candidate for connectomics approaches. It is compact and highly ordered, with a series of neuronal cell soma layers and plexiform or interconnecting layers containing repeating network motifs (Masland, 2012). Understanding how retinal neural circuits are organized, may in fact reveal general principles that neural circuits use in other nervous system tissues. Annotation and analysis of retinal connectomes is delivering a more complete understanding of the organization of neural network topology in retina than we have from any other region of the mammalian CNS.

The retina is unique in its accessibility, as gross histology, functional,

Abbreviations: RodBC, Rod bipolar cell; γAC, GABAergic amacrine cell; Aii GAC, Aii glycinergic amacrine cell; HzC, Horizontal cell; RPC1, Retinal pathoconnectome 1; RC1, Retinal connectome 1.

* Corresponding author.
** Corresponding author.
E-mail addresses: r.pfeiffer@utah.edu (R.L. Pfeiffer), bryan.jones@m.cc.utah.edu (B.W. Jones).

https://doi.org/10.1016/j.exer.2020.108196
Received 4 May 2020; Received in revised form 27 July 2020; Accepted 11 August 2020
Available online 15 August 2020

and behavioral assays can be conducted non-invasively, down to cellular resolution in living animals using optical coherence tomography (OCT) (Lujan et al., 2015) and electroretinogram (ERG) (Creel, 2019) to track the progression of disease. This accessibility is important for understanding the basic network topologies of healthy retinas in addition to dynamic processes such as development (Johnson et al., 2017; Tien et al., 2017), and how topologies are altered through aging (Samuel et al., 2011), and disease.

1.3. Neural networks in degeneration

Disruption of neural network organization leads to deficits or failures in network function (Chew et al., 2017; Day et al., 2006; delEtoile and Adeli, 2017). In a simple, static network, this is intuitive: Neuron A is presynaptic to neuron B, neuron B is presynaptic to neuron C, the loss of neuron A or B will lead to a lack of input to neuron C (Bargmann et al., 1993). These simple neural network graphs rapidly gain complexity with the addition of more neurons and associated synapses. Therefore, understanding neural networks and how changes in them contribute to the failure of appropriate network processing in neurological disease or retinal degeneration is critical for understanding the progression of these diseases (Agosta et al., 2010; Day et al., 2006; delEtoile and Adeli, 2017; Guo et al., 2015; Lacor et al., 2007). Furthermore, creating targeted therapeutic interventions to stop, reverse, modify, or interact with degenerate neural networks will depend upon understanding precisely which targets are involved in networks that are altered in disease.

1.4. Retinal degenerative disease: retinitis pigmentosa and age-related macular degeneration

Progressive neurodegenerative disease seen in retinal degenerative diseases like retinitis pigmentosa (RP) (Jones et al., 2016a) or age-related Mmcular degeneration (AMD) (Jones et al., 2016b) have many causes, but the final remodeling pathways converge on photoreceptor cell death, retinal remodeling, and often blindness. RP is a retinal disease with hallmarks of photoreceptor degeneration and subsequent neural retinal deafferentation, affecting approximately 1 in 4000 individuals (Hamel, 2006). Although over 100 genes are associated with this disease, the sequence of degeneration and clinical findings in rod dominated RP are: rod photoreceptors degenerate causing neural retinal deafferentation, loss of night and peripheral vision, followed secondarily by the degeneration of cone photoreceptors and total or near total vision loss (Hartong et al., 2006). In the retina, these negative plastic changes and cell death revise the circuit topology through a process called retinal remodeling (Jones and Marc, 2005; Marc et al., 2003) that has been observed in not only human RP, but also all models examined to date of RP, as well as human AMD. This retinal degeneration can progress to complete neurodegeneration, similar to that seen in other neurodegenerative diseases Pfeiffer et al., 2020b.

This report examines the earliest ultrastructural changes in circuitry of the retina of a model of RP, resulting in *rewiring*, which is the specific process of changes in network topology that occur through neurite outgrowth (Fariss et al., 2000; Lewis et al., 1998; Strettoi and Pignatelli, 2000), formation of new synapses (Peng et al., 2000), and loss of existing connections (Linberg et al., 2006).

1.5. Pathoconnectomics

Recent work has demonstrated that retina behaves similarly to CNS with respect to late stage disease with many of the same features observed in retina as in other neuropathies of the brain (Pfeiffer et al., 2020b). This, combined with the features that made the retina ideal for the initial mapping of neuronal networks, makes it the best candidate for mapping neuronal network disruptions that occur as a result of neurological disease. We are evaluating these disruptions by creating a series of connectomes of pathological tissue at advancing stages of degeneration: *Pathoconnectomes*. This is the first publication to our knowledge, noting the creation of pathoconnectomics approaches, or pathological connectomes of disease tissues to demonstrate how wiring is altered in models of neurodegeneration. It is our hypothesis that network changes associated with retinal degenerative disease, found in retinal pathoconectomics will expose underlying principles of negative plasticity that are generalizable across the CNS.

Our goal is to detail all of the network topologies in retina disrupted by photoreceptor degeneration. The purpose of this is two-fold: 1) To create network diagrams for better targeting of therapeutic interventions for vision loss. 2) To uncover the basic principles of neural network responses to altered or missing input. In this report, we introduce the structure, features, and initial findings from Retinal Pathoconnectome 1 (RPC1). RPC1 is an open-access, serial-section transmission electron microscopy (ssTEM) pathoconnectome volume, generated from a rabbit model of autosomal-dominant cone-sparing RP.

2. Material and methods

2.1. Model system

The retina used to generate RPC1 is from a heterozygous transgenic (Tg) P347L rabbit, which was originally generated in the Kondo Laboratory (Kondo et al., 2009). The Tg P347L rabbit has been extensively characterized and follows a pattern of progression similar to that of human cone-sparing RP (Jones et al., 2011; Ueno et al., 2019). The rabbit was 10 months old at the time of enucleation and extensive photoreceptor degeneration had begun, though the central retina still had numerous rods intact. The retina used in the control connectome RC1, was from a 13-month-old Dutch belted rabbit. The characteristics of RC1 volume have been described previously (Anderson et al., 2011a). All animal experiments were conducted according to the ARVO Statement for the use of animals in Opthalimic and Vision Research, with the approval of the Institutional Animal Care and Use Committee (IACUC) of the University of Utah.

2.2. Tissue preparation

Tissues are fixed in a mixed aldehyde solution (1% formaldehyde, 2.5% glutaraldehyde), dehydrated in graded alcohols, then embedded in epoxy resins. Tissues are then serially sectioned at 70 nm and prepared for TEM capture or CMP analysis by placing the section on a formvar grid or 12-well slide, respectively.

2.3. Image acquisition

Transmission electron microscopy (TEM) provides the high resolution required for connectomics approaches to visualize the network components, including chemical synapses and gap junctions, along with the quantitative aspects of computational molecular phenotyping (CMP) to molecularly label cell identity (Anderson et al., 2011a). These approaches have been previously used to create a healthy rabbit connectome RC1: a 250 μm in diameter volume of retina spanning from the apical inner nuclear layer (INL) to the basal ganglion cell layer (GCL), which serves as a ground truth for normal retinal circuit topology. RPC1 was constructed in identical fashion. In electron microscopy, adequate resolution is required to definitively identify all network components (2.18nm/px is the lowest resolution in which gap junctions can be positively identified) and the identification of pre- and post-synaptic structures is crucial to the accurate identification of networks. Therefore, our routine TEM acquisitions are acquired at 2.18 nm/pixel, and sections can be re-imaged at 0.27 nm/pixel, with a goniometric tilt as necessary to confirm certain circuit identities like gap junctions (Kolb and Famiglietti, 1974; Marc et al., 2018; Sigulinsky et al., 2020).

2.4. Volume assembly and annotation

Serial TEM images were acquired on a JEOL JEM-1400 electron microscope with a 16-Mpixel Gatan camera, while CMP images were acquired using a Leica light-microscope affixed with 8-bit CCD camera. RPC1 was assembled using the custom Nornir tools developed for volume assembly. Nornir combines individual images acquired from transmission electron microscopy or from a light-microscope, and registers individual image tiles into assembled mosaics before using automated registration to align adjacent sections throughout the volume, with minimal manual correction (Anderson et al., 2009; Marc et al., 2012). Following volume assembly, navigation and annotation of the dataset is performed in the Viking software environment (Anderson et al., 2011b). Annotation of every chemical or electrical synapse type is made to avoid false positives of connectivity and minimize missed structures. For further description of synapse identification metrics used in this study, see Supplementary Figs. S1–S3.

2.5. Computational molecular phenotyping (CMP)

Along with ultrastructural data, molecular tagging of cellular identity is fundamental to understanding contributors to neuronal networks. CMP allows for cell classification through quantitatively evaluating the combinations of small molecules, which are stoichiometrically trapped during fixation (Marc and Cameron, 2002; Marc et al., 1995; Ottersen, 1989), and detected with glutaraldehyde-tolerant IgGs. The concentrations of the probed amino acids and proteins are used in the identification of cells beyond their morphology and synaptology (Table 1). For more in depth information on CMP technologies and usage see (Marc and Jones, 2002Marc et al., 1995; Pfeiffer et al., 2020a). Small molecule IgGs to GABA, L-glutamate, L-glutamine, glycine, and taurine, in addition to IgGs targeting glial fibrillary acidic protein (GFAP) were used in the classification of cells in the RPC1 volume.

2.6. Viking software

Viking annotations encode information about the size, structure, and location of all annotated structures within connectomes and pathoconnectomes, facilitating database-base queries of parameters including statistics of encoded structures (Anderson et al., 2011b; Marc et al., 2012). These databases are publicly accessible at www.connectomes.utah.edu and http://websvc1.connectomes.utah.edu/RPC1/OData.

2.7. Figure assembly

Figures were assembled using screenshots from the RPC1 volume in Viking (http://connectomes.utah.edu/, RRID:SCR_005986), 3D renderings of cells were generated in VikingView (https://doi.org/10.5281/zenodo.3267451, https://zenodo.org/record/3267451#.XSUW1OhKguU), and whole volume renderings were generated in Blender (http://www.blender.org/; RRID: SCR_008606). Final figure assembly was done in Photoshop 6.0.

Table 1
Immunocytochemistry reagents.

Reagent	RRID	Source	Dilution
anti-L-glutamate IgG	AB_2532055	Signature Immunologics	1:50
anti-glycine IgG	AB_2532057	Signature Immunologics	1:50
anti-L-glutamine IgG	AB_2532059	Signature Immunologics	1:50
anti-taurine IgG	AB_2532060	Signature Immunologics	1:50
anti-GABA IgG	AB_2532061	Signature Immunologics	1:50
anti-GFAP	AB_10013382	Dako	1:200

3. Results

3.1. Retinal pathoconnectome 1 (RPC1)

RPC1 is composed of 946 serial TEM sections with 14 intercalated IgG probes generated against small molecules important in metabolism (Fig. 1). In this volume, 1 out of 30 sections cut were placed on slides for Computational Molecular Phenotyping (CMP) probing, while the other sections were placed on formvar grids for ssTEM imaging. The RPC1 volume is narrower in diameter (70 μm) than our control RC1 volume (250 μm), allowing for more rapid capture and assembly, while still large enough to capture repeated rod-network motifs (Lauritzen et al., 2019). RPC1 is the first pathoconnectome volume in a series of 3, each with increasingly severe photoreceptor degeneration (with eventual neurodegeneration in later timepoints) to chronicle landmarks in rewiring as the disease progresses (For more complete description of disease progression in the Tg P347L retina, please see Pfeiffer et al., 2020b or Jones et al., 2011). RPC1 derives from a 10-month-old Tg P347L rabbit retina, model of RP (see methods). In the selected region of retina (peri-visual streak), photoreceptor degeneration had initiated and the outer nuclear layer (ONL) was reduced in thickness by approximately 50% (Fig. 1A). Though rod photoreceptors were the most heavily degenerated neuronal class, many rods remain morphologically intact. The remaining rod photoreceptors, along with the inner retinal cell population, allowed for connectomics-based evaluation of early-stage RP rewiring, corresponding to a clinical point where human patients would still have vision, though would likely be suffering from scotopic deficits as well as adaptation deficits. In total, 321 neuronal and glial somas have been identified within the volume and assigned to broad classes in RPC1. The breakdown of cells is as follows: 113 photoreceptors, 5 horizontal cells, 81 amacrine cells, 79 bipolar cells, 4 ganglion cells, at least 36 Müller glia, and 4 microglia. Examination of these cell classes has revealed altered network topologies associated with rewiring in early photoreceptor degeneration, *prior to* complete rod degeneration or inner retinal neuronal loss.

3.2. Rod-network pathologies

Rod photoreceptors are the first cells in this heterogeneous neuronal network to degenerate. Therefore, the first network we sought to characterize in RPC1 was the rod-mediated network. The literature of retinal networks is vast, so only a simplified description of the rod-network is provided below along with a graphical description (Fig. 2). For more comprehensive descriptions of additional retinal networks see: (Diamond, 2017; Lauritzen et al., 2019; Marc et al., 2014; Marc et al., 2018; Thoreson and Dacey, 2019).

Rod photoreceptors (rods) are specialized neurons responsible for detection of photons in low-light (scotopic) conditions. Following photon capture, rods initiate an enzymatic cascade ultimately leading to a hyperpolarization. This hyperpolarization causes a decrease in glutamate release into the synaptic cleft, signaling to postsynaptic rod bipolar cell (RodBCs) dendrites, via the first synapse in vision located in the outer plexiform layer (OPL). Axons of RodBCs branch and synapse in the deepest layer of the inner plexiform layer (IPL), close to, but not connecting with ganglion cells in the ganglion cell layer (GCL). RodBCs are presynaptic to at least 2 classes of amacrine cells: GABAergic amacrine cells (γACs) and Aii glycinergic amacrine cells (Aii GACs). Aii GACs are chemically presynaptic to OFF cone bipolar cells (OFF CBC) using the neurotransmitter glycine, causing inhibition. However, in the ON-layer, Aii GACs make gap junctions with ON cone bipolar cells (ON CBCs), sharing their polarization state through these gap junctions with the ON CBCs. ON CBCs in turn synapse with ganglion cells that ultimately project out of the retina, and into the brain via the optic nerve, thereby passing the rod signal out of the retina. In healthy retina, RodBCs are never presynaptic to ganglion cells and therefore “piggyback” on the ON CBC pathway using the Aii GAC as described above. This rod pathway is

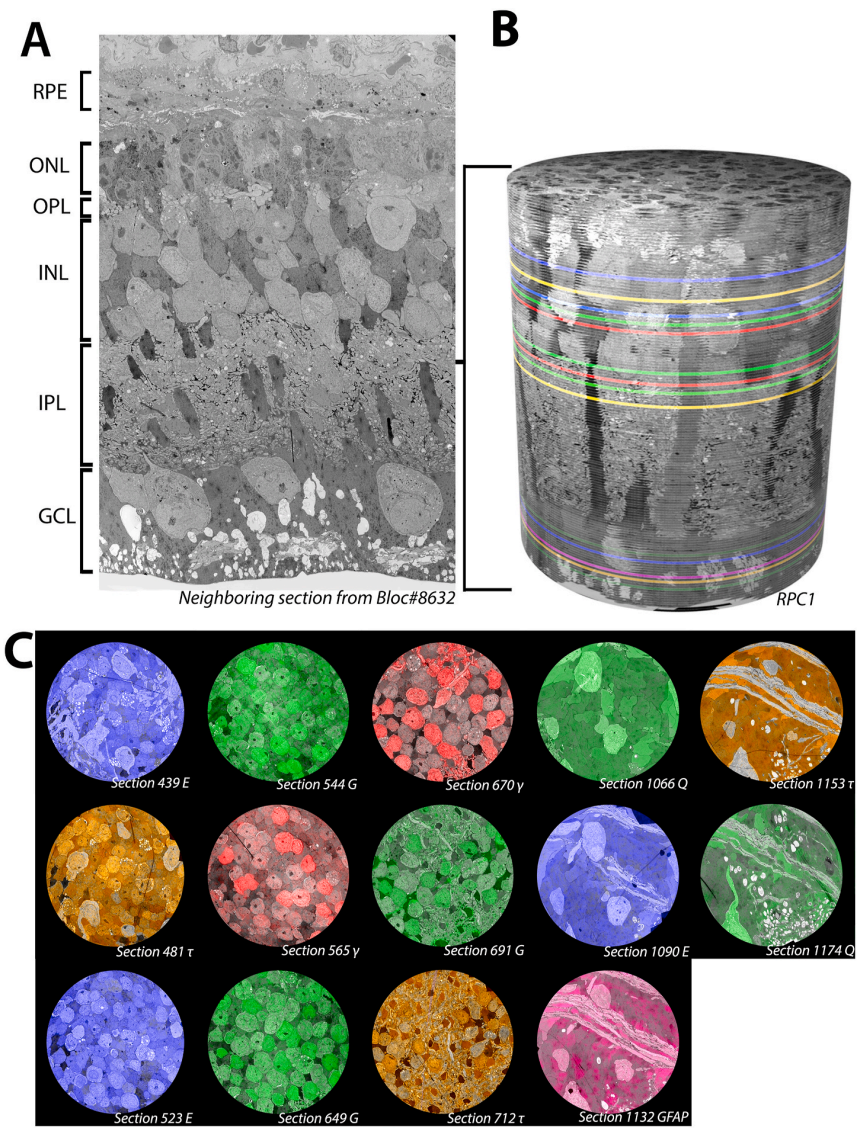

Fig. 1. Overview of RPC1. (A) Vertical section through tissue directly adjacent to the tissue processed for the RPC1 volume. (B) 3D composite volume of RPC1. Pseudocolored sections illustrate the locations of CMP sections for small molecules indicated in 1C. (C) Overlaid CMP sections from RPC1 on their adjacent TEM sections. Letters indicate probes used: Glutamate (E), Taurine (τ), Glycine (G), GABA (γ), Glutamine (Q), and glial fibrillary acidic protein (GFAP).

highly conserved and observed in all mammalian retinas.

3.2.1. *RodBC outer plexiform layer pathology*

RPC1 contains 17 RodBCs, 8 of which have axonal and dendritic arbors contained entirely within the volume. RodBCs are traditionally thought to be exclusively postsynaptic to rod photoreceptors in the healthy retina. In contrast, recent studies have proposed that RodBCs may be post-synaptic to cones in addition to rods in healthy retina. In evaluating these studies, we find the resolution and lack of clear post-synaptic densities to the cone pedicles make it difficult to determine whether the RodBCs are truly synapsing with the cone pedicle or merely traversing in close proximity (Behrens et al., 2016; Pang et al., 2018). Because our RC1 volume does not include an OPL, we could not directly assess whether these contacts exist using our identification metrics, though the serial TEM reconstruction of RodBCs in a healthy mouse by Tsukamoto and Omi failed to identify any cone inputs to these cells (Tsukamoto and Omi, 2013). In photoreceptor degeneration retinal diseases however, it is widely accepted that RodBCs retract their rod-contacting dendrites as rods die and extend new neurites towards cone pedicles making peripheral contacts (Peng et al., 2000). In evaluating the OPL of RPC1, we found this process initiates prior to complete rod degeneration. 7 RodBCs maintained contact with existing rods, while many simultaneously demonstrated aberrant contacts with cones or indeterminate photoreceptors (Fig. 3A). We observed 12 RodBCs post-synaptic to cone photoreceptors, with 4 of those cone-contacting RodBCs maintaining at least 1 post-synaptic density to a rod axon terminal (spherule) (Table 2). Though most cone-contacts are with traditional cone axon terminals (pedicles) (Fig. 3B), we found one instance of a sprout off the primary pedicle with a secondary terminal presynaptic to RodBC 822 (Fig. 3B+E). We found an additional 12 RodBCs with densities opposing non-traditional structures containing ribbons (Fig. 3F). In these cases, we found 1 RodBC opposing axonal ribbons and no terminal, and 11 opposing ribbon terminals inconsistent with morphology typically associated with rod spherules or cone pedicles and

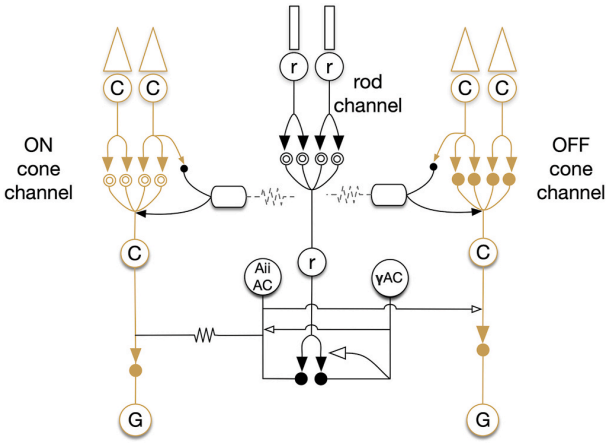

Fig. 2. Simple diagram of rod bipolar cell network. Solid arrows indicate glutamatergic synapses. Open arrows indicate inhibitory synapses (GABA or glycine). Solid circles indicate ionotropic glutamate receptors, while mGluR6 is indicated by the double open circles. Gap junctions are indicated by zig-zag lines.

could not be conclusively morphologically classified as a rod or cone terminal. Because 9 of the RodBC dendritic arbors evaluated are not entirely contained within the volume, the number of cone contacts made by RodBCs in RPC1 may be greater than the currently tabulated 70.5% (12/17). These results confirm previous light microscopy work indicating RodBCs extend neurites to cone pedicles as the rod photoreceptors degenerate, and expands upon this by determining RodBCs extend neurites towards cone pedicles prior to becoming fully deafferented from rod spherules. For complete list of RodBC photoreceptor contacts see Table 2.

3.2.2. *RodBC inner plexiform layer pathology*

We then compared the inner retinal network of RPC1 with the previously described IPL network topologies of RC1 to determine the potential network impacts of changes in RodBC inputs. RodBCs are typically only associated with chemical synapses within the IPL. Specifically, RodBCs in the healthy retina are found presynaptic via glutamatergic ribbon synapses to Aii GACs and yACs. We found the total ribbon synapses made by complete RodBCs of RPC1 ($n = 8$) were similar to representative RodBCs ($n = 5$) from RC1. RPC1 ribbons: 34.125 ± 4.29 (mean $\pm$ standard deviation) and RC1 ribbons: 34.4 ± 2.5 ($p = 0.8$, unpaired Student's-t-test). Although the numbers of ribbon synapses were not altered, some ribbon synapses of bipolar cells, including RodBCs, were morphologically altered. Rather than the typical "bar" shaped ribbons (Fig. 4A), a subset of ribbons ($n = 16$) had a spherical morphology (Fig. 4B + C) commonly associated with immature or disassembling ribbon synapses (Adly et al., 1999; Spiwoks-Becker et al., 2004; Strettoi et al., 2002). In addition to their presynaptic signaling, RodBCs are also heavily postsynaptic to inhibitory synapses from yACs (Lauritzen et al., 2019). The prevalence of postsynaptic densities was also similar between RPC1: 69.625 ± 14.050 and RC1 62.8 ± 13.498 ($p = 0.406$, unpaired Student's-t-test). These results suggest that chemical synapse numbers are not substantially changed at this early stage of photoreceptor degeneration. For complete list of RodBC synapses see Table 2.

Chemical synapses between RodBCs, Aii GACs, and yACs appear to be largely intact in the early degenerate retina and occur in similar frequency to that observed in healthy retina. However, we observed the emergence of gap junctions involving RodBCs of RPC1. In the adult healthy mammalian retina, RodBCs do not make gap junctions. This is confirmed in our RC1 volume, where none of the 104 RodBC axonal arbors are found to contain a single gap junction (Sigulinsky et al., 2020). In contrast, all 17 RodBCs found within RPC1 formed at least 1 gap junction. In total, we have identified 50 candidate gap junctions, 18 of which were confirmed using high magnification (0.43nm/pixel) and goniometric tilt (Fig. 5), which revealed the confirmatory pentalaminar structure associated with gap junctions. At least one gap junction per RodBC was confirmed using high magnification with the exception of RodBC 26167, which is largely off volume and recapture was not possible of its only identified candidate gap junction. Next, we identified gap functionally coupled partners of these RodBCs. No gap junctions were found between paired RodBCs in RPC1, despite substantial overlap of arbors in some areas (Fig. 5C). Of the 50 gap junctions, 48 (96%) were positively identified with Aii GACs. In all cases of gap junctions with Aii GACs in RPC1, the individual RodBC was also heavily presynaptic to the same Aii GAC via glutamatergic ribbon synapses, often within the same varicosity as the gap junction. Of the gap junctions not made with a confirmed Aii GAC, 1 was with an unidentified partner, which could not be conclusively identified due to being near the volume edge. The other non-Aii GAC partner was an ON CBC. These data demonstrate that RodBCs, early in the retinal degenerative process, alter their inner retina synaptology through the formation of gap junctions, especially with Aii GACs, though chemical synaptology remains intact. There also appears to be preferred class-specific partnering via gap junctions that may reveal the presence of cell-cell markers or targets for therapeutic intervention. What implications this has for network performance or stability is currently unclear, but is an area of future modeling work.

3.3. *GABAergic amacrine cell neurite sprouting*

There are 31 identified and annotated GABAergic amacrine cell (γAC) somas contained within the RPC1 volume. In the healthy retina, γACs (with the exception of some starburst amacrine cells) have a soma that is predominately positioned within the INL just apical to the IPL, with processes extending solely into the IPL. Within the IPL yACs make conventional inhibitory chemical synapses with multiple partners, and some classes are also known to make extensive gap junctions with other yACs and certain classes of ganglion cells (Marc et al., 2018). All 107 γACs contained within RC1 are consistent with this description.

Conversely in disease, prior work has demonstrated that processes of γACs can be found extending apically towards the OPL during photoreceptor degeneration (Jones et al., 2011). However, it was unclear whether these GABAergic processes were neurites that extended off of the normal processes below the soma before extending apically, or whether they arose from the soma itself. In RPC1, 4 of the 31 γACs were found to extend processes from the apical side of their somas into the OPL (γAC cell #s: 769, 993, 997, and 2627) (Fig. 6). Not only is this confirmatory at ultrastructure of the previously described novel GABAergic processes in the OPL, but demonstrates that the extension of these processes arises from the soma, and manifests prior to complete loss of rods. We then analyzed the synaptic connections made by these aberrant apical processes and found chemical synapses in the OPL made by these γAC neurites. However, the number of synapses and their pre- and post-synaptic partners was variable. γAC 769 extended into the OPL, but made no identifiable synapses. Conversely, γAC 993 was the most complex of these apical extending processes. γAC 933 made 6 synaptic contacts in the OPL: 2 postsynaptic densities to conventional synapses originating from horizontal cells and 4 synapses in which γAC 993 was presynaptic to multiple classes of ON bipolar cells, creating a novel 2-hop inhibitory network between horizontal cells and ON bipolar cells. γAC 997 was postsynaptic to a single horizontal cell, and γAC 2627 was presynaptic to a horizontal cell and an OFF bipolar cell. These connectivities are novel in 2 distinct ways: 1) γACs in RPC1 make typologically correct contacts with bipolar cells, even when encountered in the wrong lamina. 2) γACs make aberrant synapses with horizontal cells that they never come in physical proximity with in the healthy retina, potentially affecting center-surround inhibition created by the horizontal cells. This demonstrates the ability of deviant processes that infiltrate an aberrant

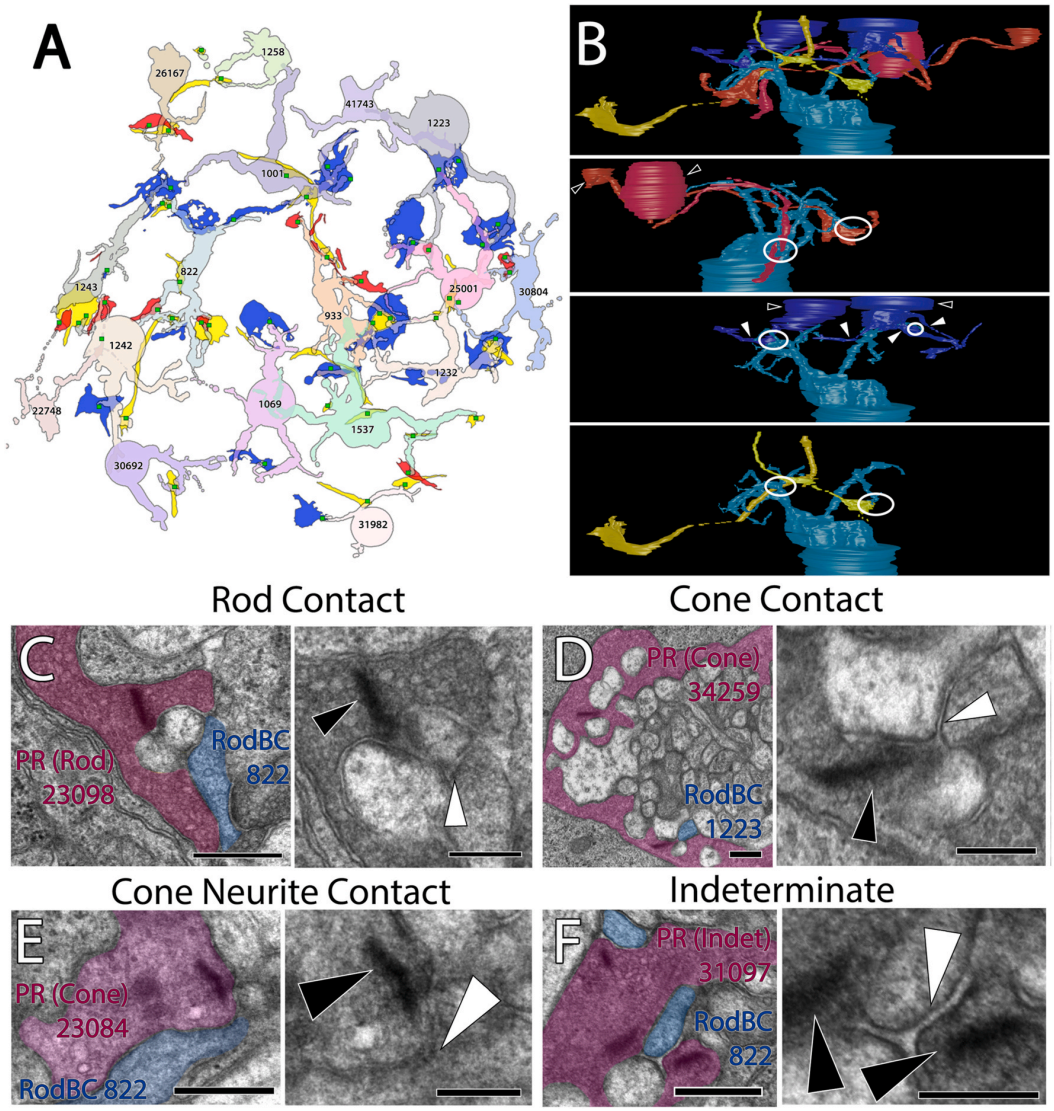

Fig. 3. RodBC dendritic contacts. (A) 2D projection image of RodBC dendrites and their synapse locations with rod (red), cone (blue), and indeterminate (yellow) photoreceptors. Ribbon locations are represented by bright green squares. (B) 3D morphology renderings of RodBC (teal) 822's synapses with rod (red), cone (dark blue), and indeterminate (yellow) photoreceptors. Location of ribbon synapses are indicated by white spheres. Cell bodies are indicated hollow arrows and neurites are indicated with solid arrows. *Note: Rotation is altered between photoreceptor type to allow for best view of synapse locations.* (C) Representative rod photoreceptor synapse of RodBC 822 postsynaptic to rod 23098. (D) Representative cone photoreceptor synapse between a cone photoreceptor 34259 and RodBC 1223. (E) Representative photoreceptor synapse between 23084 cone neurite ribbon and RodBC 822 (F) Representative photoreceptor synapses between an indeterminate photoreceptor 31097and RodBC 822. Black arrowheads indicate ribbon densities, while white arrowheads indicate associated post-synaptic densities. *Pseudocolored Images Scale bars* 500 nm. *Higher Magnification Scale Bars* 250 nm.

layer to make synapses with numerous typologically correct and incorrect partners, clearly altering the neural networks downstream of cells actively undergoing degeneration.

4. Discussion

Rewiring of neural networks through plasticity mechanisms is a prominent consequence of injury or disease in the central nervous system. Multiple studies have explored the mechanisms of neurite outgrowth (Lin et al., 2012), localized the sites of projections (Fisher et al., 2005; Peng et al., 2000), and identified a subset of synaptic partners (Fisher et al., 2005; Morimoto et al., 2004; Schmid et al., 2016). Unfortunately, exploring this using antibody probes relies on pre-existing expectations of proteins that may be involved. In addition, even when the correct protein is predicted, many synaptic structures underlying networks are too small to resolve in light microscopy or lower resolution electron microscopy approaches. Ultrastructural pathoconnectomes captured at 2nm/pixel allows for exploration and characterization of these novel networks formed by native neurons and aberrant neurites to establish precise wiring topologies, as well as identify potential rulesets that neural tissues undergoing degeneration may adopt. These networks also identify targets for potential therapeutic intervention.

In RPC1, this region of retina still contains both cones and a substantial population of rod photoreceptors. Therefore, this region would likely still exhibit both photopic and scotopic light responses, but might

Table 2
RodBC synaptic contacts.

ID	Label	Ribbons	Gap Junctions	Rod Input	Cone Input	Indeterminate Input	IPL Inhibitory PSDs	Fully contained in volume
822	RodBC	38	4	2	2	5	93	y
933	RodBC	35	2	3	2	3	62	y
1001	RodBC	31	3	0	3	2	70	y
1069	RodBC	32	7	0	2	1	61	y
1223	RodBC	21	2	0	2	0	32	n
1232	RodBC	35	3	0	4	3	62	y
1242	RodBC	25	1	0	1	1	70	n
1243	RodBC	27	6	0	2	2	56	y
1258	RodBC	27	2	0	0	2	56	n
1537	RodBC	34	3	1	1	4	89	y
22748	RodBC	20	3	2	0	1	38	n
25001	RodBC	41	4	1	2	0	63	y
26167	RodBC	16	1	1	0	0	53	n
30692	RodBC	15	1	0	0	1	28	n
30804	RodBC	32	4	2	0	2	57	n
31982	RodBC	17	1	0	1	2	22	n
41743	RodBC	26	5	0	1	0	61	n

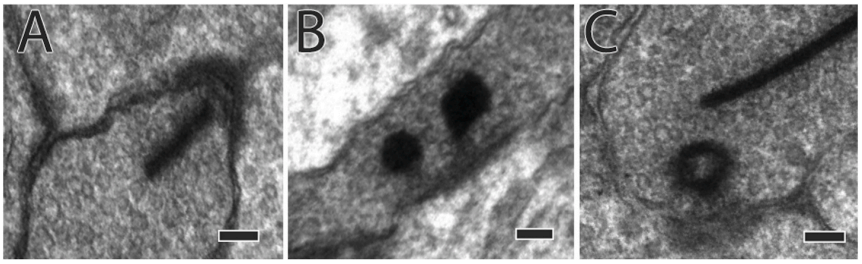

Fig. 4. Spherical Ribbons in RodBCs of RPC1. (A) Example normal ribbon made by RodBCs. (B) 2 example spherical ribbons. (C) The hollow conformation of spherical synapses. *Scale bars:* 100 nm.

have difficulty adapting between the two environments given corruption of the rod network through the introduction of gap junctions. These findings support clinical observations in patients undergoing early stages of progressive retinal degenerative diseases (Kalloniatis and Fletcher, 2004). Our observations of changes in the rod pathway and γAC connectivities are important contributing components to understanding the progression of retinal degenerative disease, and are fundamentally important to implementing therapeutic interventions. It is crucial to note that these network revisions are occurring prior to substantial inner retina neuronal cell loss, and certainly prior to the network completely failing.

RodBCs retract processes away from rod photoreceptor terminals (while maintaining contact with others) and instead contact cone pedicles in addition to apparent neurites off of cone pedicles. This possibility was suggested from earlier studies, but the precise connectivity required connectomic analysis. Beier and colleagues demonstrated in 2017, that following laser ablation of rod photoreceptors, RodBCs would extend new processes to rods still intact at the edge of the ablation zone (Beier et al., 2017). These results demonstrate deafferented RodBCs do search for new photoreceptor inputs, though in this study it was concluded that there is a preferential selection for rod photoreceptor terminals when they are available. Our findings indicate that while rods are likely still the preferred input for RodBCs, they will begin making aberrant synapses with cone terminals prior to the complete loss of available rods, including with neurite sprouts off of existing cone terminals. Prior studies by Fei et al. and Lin et al. 2009, demonstrated cone neurite sprouting in late retinal degeneration following substantial cone degeneration (Fei, 2002) and the initiation od cone remodeling in rd1 mice by pnd 8, with cone sprouts visible by pdn 25 (Lin et al., 2009). However, we find this process initiates early in photoreceptor degeneration, prior to the complete loss of rod photoreceptors and onset of cone degeneration. Also, in 2017 work from the Kerschensteiner group demonstrated high plasticity in RodBCs where following partial ablation of RodBCs, the surrounding RodBCs will expand their dendritic and axonal territories to fill the gap (Johnson et al., 2017). We find no clear morphological changes in the axons of the RodBCs of RPC1, however, we also do not observe a clear decrease in RodBC packing density. It is possible this phenomenon will emerge in future pathoconnectomes of more advanced retinal degeneration as inner retinal cell death initiates. Finally, the plasticity of the RodBCs and their ability to restore some afferent input during photoreceptor degeneration is likely also related to the age of the animal. The Kerschensteiner group recently published a study describing the plasticity of cone bipolar cells in restoring afferent input at different ages (Shen et al., 2020). This study found that most ON-cone bipolar cells most lose plasticity required to completely restore proper inputs as the animal ages. While they did not explicitly investigate RodBCs, it is likely that age of the animal plays a role in the RodBC plasticity and ability to restore the same levels of afferent input should rod degeneration be halted or therapeutically restored. Our results extend our knowledge of RodBC inputs during early retinal degeneration and indicate that early in retinal degeneration there is mixing of the rod and cone inputs through the RodBCs.

Although the numbers of ribbons and gross morphology of the RodBC axons were similar between RodBCs of RPC1 and RC1, the spherical ribbon synapses were unique to RPC1, and their altered morphology origins could be complex. With respect to retinal degeneration, Strettoi et al. described ribbons with similar morphology in the RodBCs of postnatal day 30 (pnd30) rd1 mice (Strettoi et al., 2002). At this time point, photoreceptors are largely degenerated and RodBCs never fully develop due to the rapid onset and progression of photoreceptor degeneration in this model. Based on this and morphological similarities between ribbons in pnd30 rd1 mice, and developing ribbons, Strettoi and colleagues proposed that the spherical ribbons were due to lack of complete RodBC development in this model. In the P347L

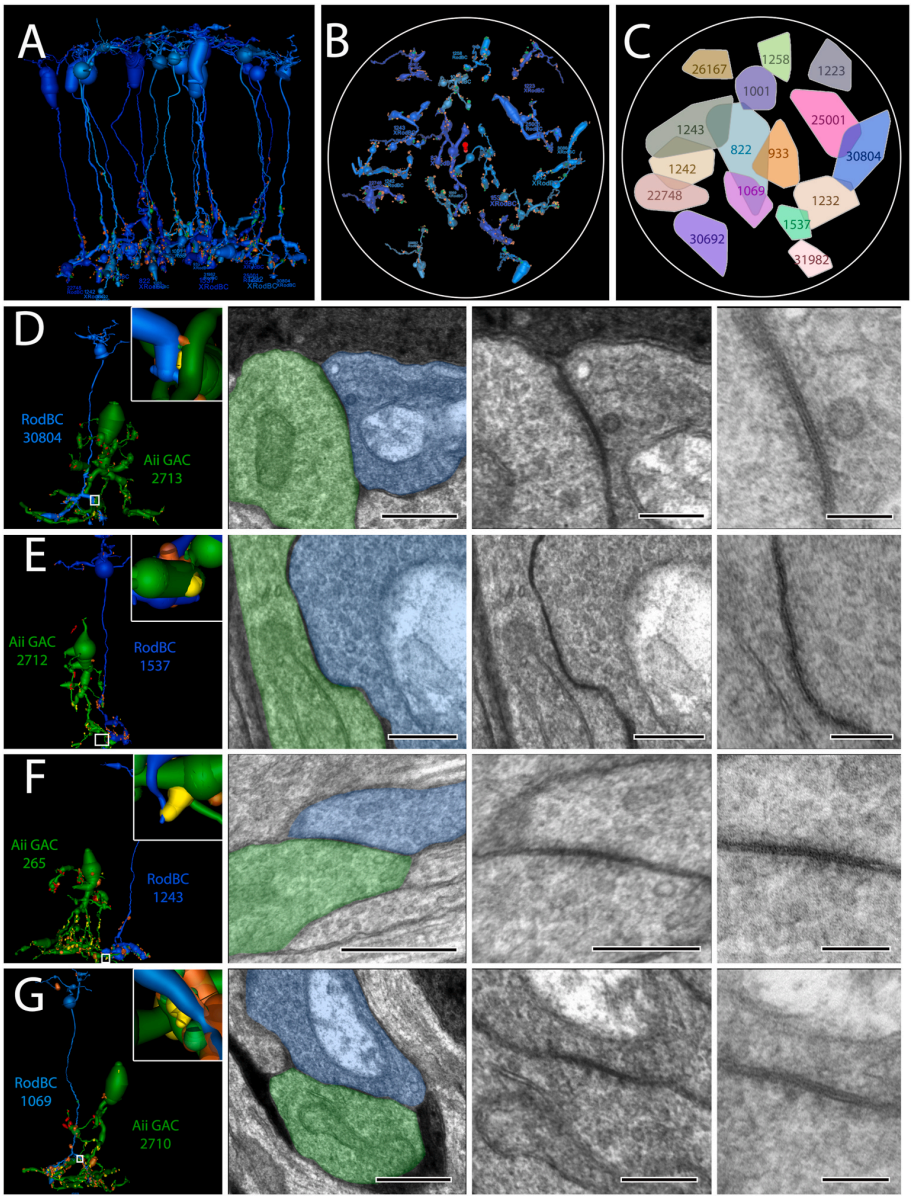

Fig. 5. RodBC gap junctions with Aii GACs (A) 3D rendering of all 16 RodBCs from RPC1. (B) RodBC axonal arbor fields in RPC1. (C) Convex Hulls of all RodBCs in RPC1 (D–E) Gap junctions between RodBCs and Aii GACs. Left panel is 3D rendering with inset higher magnification image of specific gap junction annotations. White boxed image corresponds to white box in adjacent left panel. * indicate ribbons and # indicates gap junctions arising in same varicosity. 100 nm scale images are 25 k recaptures of gap junction structures.

transgenic model, lack of complete development is not a confounding feature, the Tg P347L rabbit retina fully develops and does not initiate degeneration until approximately 3 months of age (Jones et al., 2011; Kondo et al., 2009). Further suggesting photoreceptor degeneration as an initiating cause of abnormal ribbon morphology, a recent publication by Strettoi and colleagues demonstrates the appearance of spherical (they term globular) ribbons following photoreceptor degeneration in a photoinducible (I307N) retinal degeneration mouse model (Stefanov et al., 2020). Spherical ribbons, however are not isolated to the developing or degenerating retina. Vollrath and colleagues demonstrated the presence of spherical synaptic bodies in photoreceptor terminals appearing coordinated with time of day and illumination of the photoreceptors and are associated with the shortening and lengthening of photoreceptor terminal ribbons. A greater number of spherical bodies near ribbon synapse sites appear in the middle of the subjective day, and are largely abolished during subjective night, and in continuous darkness (Adly et al., 1999; Spiwoks-Becker et al., 2004). In addition, Schmitz, confirmed the findings of Vollrath and colleagues while adding the hypothesis that decreasing levels of intracellular calcium may be contributing to the disassembly of photoreceptor ribbon synapses during high illuminance (Schmitz, 2014). Combined, these studies suggest a number of mechanisms that may be contributing to observations of spherical ribbons in degenerate retina. We have previously hypothesized that features of photoreceptor degeneration, leading to less bipolar cell input, combined with features of remodeling such as the decrease of mGluR6 expression (Jones et al., 2011; Marc et al., 2007; Strettoi and Pignatelli, 2000) may be leading to changes in calcium levels of inner retinal neurons along with altered gene expression (Jones et al., 2012; Marc, 2010; Marc et al., 2007). Extending this hypothesis, we propose that the observed spherical ribbons may be a result of decreased intracellular calcium in the bipolar cells, occurring by a similar mechanism to that observed in photoreceptors.

Central to connectomics analyses, specificity in synaptic partners is critical to the function of a neural network. Many complex feedforward

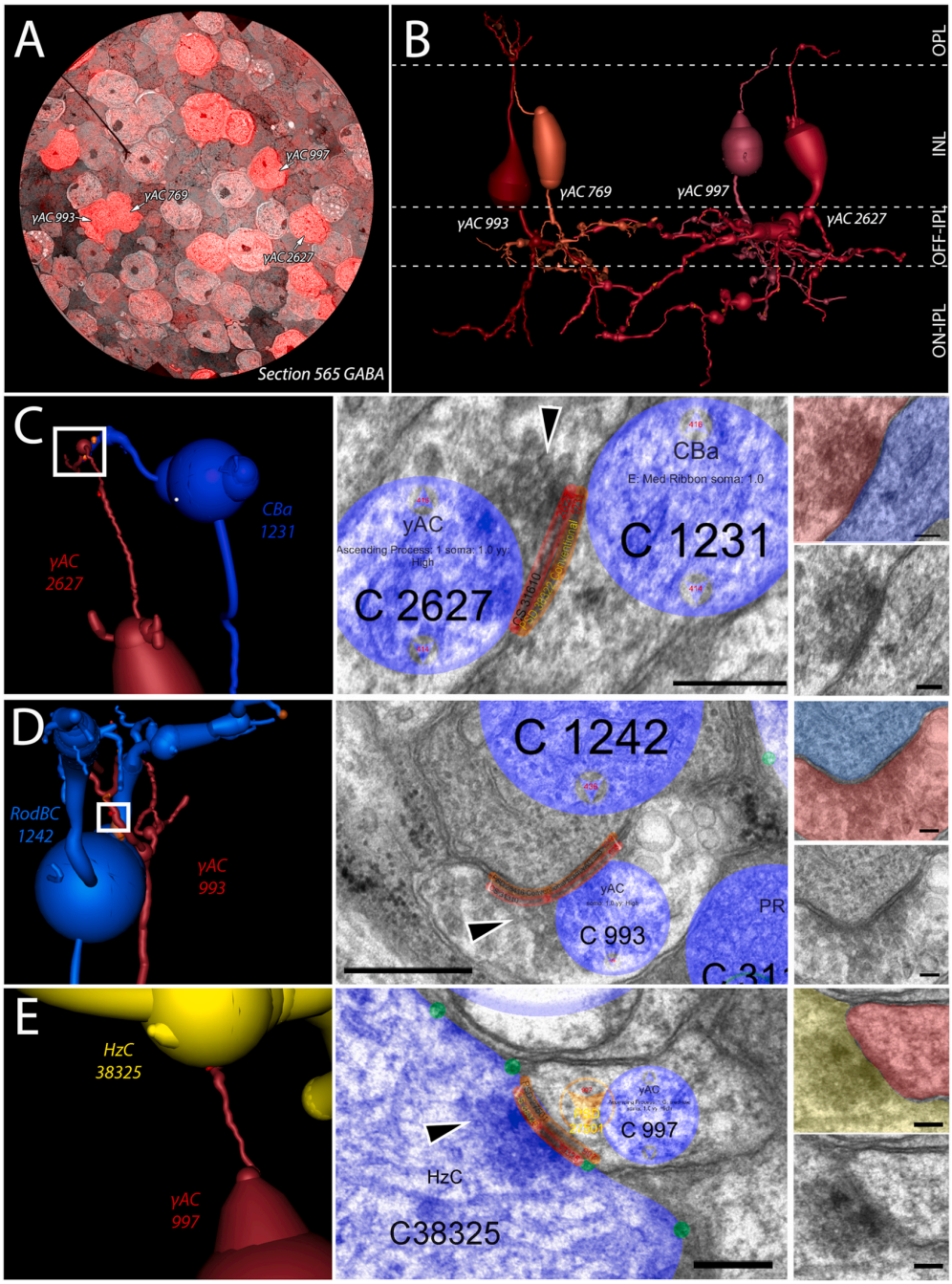

Fig. 6. Ascending process of GABAergic amacrine cells. (A) CMP overlay of GABA section 565 on its neighboring TEM section. Intensity of red color indicates higher levels of GABA contained within the cell. (B) 3D rendering of the 4 γACs with ascending processes in RPC1. (C) Synapse between γAC 2627 and OFF-BC 1231 in the OPL. White box indicates region of synapse shown on the right in increasing magnification. Black arrowhead indicates the presynaptic vesicle cloud. (D) Synapse between γAC 993 and RodBC 1242 in the OPL. White box indicates region of synapse shown on the right in increasing magnification. Black arrowhead indicates the presynaptic vesicle cloud. (E) Synapse between γAC 997 and HzC 38,325 in the OPL. White box indicates region of synapse shown on the right in increasing magnification. Black arrowhead indicates the presynaptic vesicle cloud. *Scale bars:* 250 nm *(Viking annotated)* 100 nm *(smaller inset)*. (For interpretation of the references to color in this figure legend, the reader is referred to the Web version of this article.)

and feedback loops have emerged as underlying properties long observed in physiological studies. For example, psychophysical studies of vision prompted many hypotheses of crossover inhibition between networks (Buck, 2014, 2004; Stabell and Stabell, 2002), which were later specifically defined using connectomics (Lauritzen et al., 2019). The present pathoconnectome reveals the early onset of network-level changes involved in the breakdown of primary visual pathways within the retina (Fig. 7). The emergence of gap junctional coupling between RodBCs and Aii GACs contributes to the deterioration of the rod-network prior to the complete degeneration of the rod photoreceptors and likely

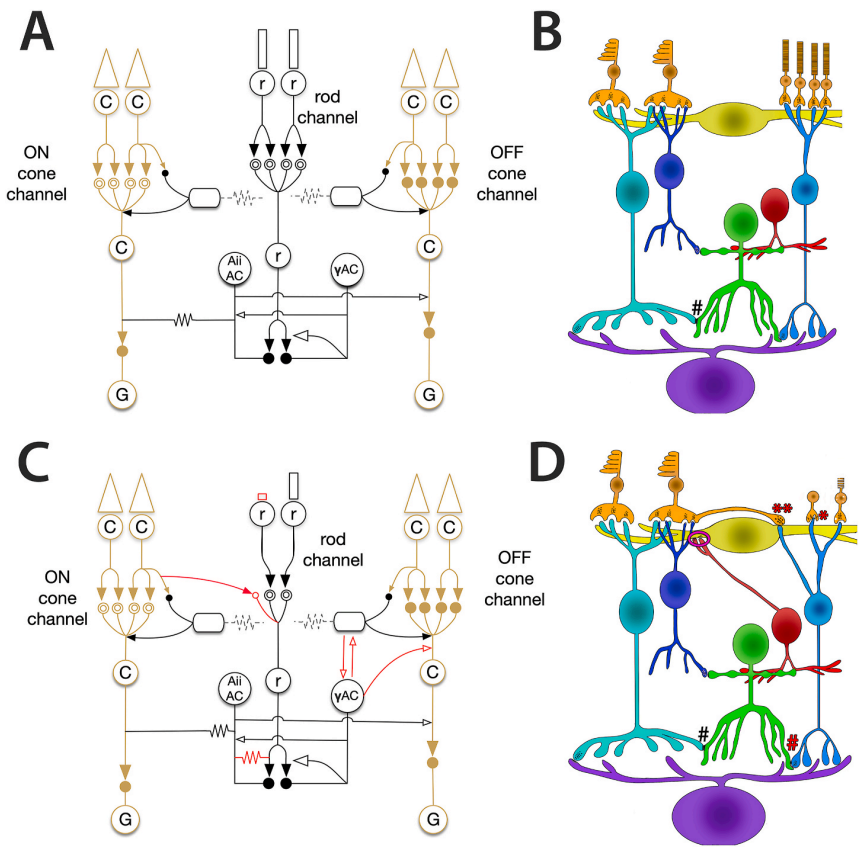

Fig. 7. Altered network found in RPC1. (A-B) Phase 0 (Healthy) bipolar cell network (A) Schematic network diagram highlighting connectivity evaluated in RPC1. Solid arrows indicate glutamatergic synapses. Open arrows indicate inhibitory synapses (GABA or glycine). Solid circles indicate ionotropic glutamate receptors, while mGluR6 is indicated by the double open circles. Gap junctions are indicated by zig-zag lines. Red lines indicate aberrant connectivities observed in the RPC1 volume. (B) Illustration of RodBC network in healthy retina. # highlights gap junction between Aii GAC and ON cone bipolar cell. (C-D) Phase 1 corrupted network. C) Schematic diagram of remodeled network found in RPC1. Notation is the same as used in A with the addition of red arrows highlighting the corrupted network components observed in RPC1. (D) Illustration of cell connectivity changes observed in RPC1. Magenta ellipsoid highlights addition of contacts between HzCs and the apical neurite off of γAcs. Red # indicates the novel gap junction formed between Aii GACs and RodBCs. Red * indicates the indeterminate photoreceptor inputs to RodBC dendrites. Red ** indicates the inputs to Rod BC dendrites from cone neurite sprouts.

compromises the spatial and temporal resolution found in the intact network. Direct questions that these results pose are: How do RodBCs which in healthy mammalian retina do not form gap junctions, form them during retinal degeneration, and what are the connexins involved? These questions require more experiments to completely answer, however some predictions can be made. John O'Brien's group demonstrated the presence of sparse, small, gap junctions utilizing connexin 35 (mammalian Cx36 homolog) in the in PKCa-positive Mb1 bipolar cells (RodBCs) of bass retina (O'Brien et al., 2004). Recent results have also demonstrated an increase in Cx36 expression in the IPL of degenerating adult mouse retina (Stefanov et al., 2020).Though gap junctions have not been observed in RodBCs of the mammalian retina, this demonstrates the evolutionary possibility of their expression under the right conditions. Such conditions may include the widespread phenotypic switching (Jones et al., 2011, Marc et al., 2007) and gene expression changes (Hackam et al., 2004) that are observed in retinal degeneration. Future in-depth immunohistochemistry and genetic studies will be necessary to pinpoint the connexins involved and the mechanisms by which they are expressed.

Furthermore, though the vertical pathway of rod photoreceptors to RodBCs is unsurprisingly altered, we find the extent of changes in the horizontal pathway especially interesting. Apical neurites from γACs, not only extend and traverse the OPL, but also make anatomically confirmed synapses with bipolar cells in addition to horizontal cells. Both horizontal and amacrine cells are integral to creating the center-surround opponency essential for complex vision. One possibility is that these are actually interplexiform amacrine cells that have been described across species since the 1970's (Dowling and Ehinger, 1975, Oyster and Takahashi, 1977). However, the exact classification of these neurons has been a difficult problem in retinal circuitry literature. Some publications have described these as being either glycinergic or dopaminergic in the goldfish (Kalloniatis and Marc, 1990), though we only find these processes extending from GABAergic cells. Other studies find interplexiform amacrine cells may be GABAergic in mouse (Dedek et al., 2009), but find much larger associated arbors in the ON-layer of the IPL than what we observe here. In the rabbit, interplexiform amacrine cells have been observed at a much lower density than what we find in RPC1 as well as having a different morphology (Oyster and Takahashi, 1977). Therefore, we believe the most probable source of these ascending processes is due to sprouting initiated by the remodeling rather than finding an interplexiform amacrine cell subtype not observed in RC1, though we cannot rule out the possibility. The novel electrical synapses formed by the emergence of gap junctions between RodBCs and Aii GACs, creates a new feedback loop with RodBCs rather than the unidirectional RodBC to Aii GAC pathway observed in healthy retina. In addition, the sprouting of horizontal and amacrine cells in various models of photoreceptor degeneration has been well documented (Fisher et al., 1995; Jones et al., 2003; Strettoi and Pignatelli, 2000), in this report we find this is occurring substantially before rod photoreceptors are completely degenerated. The new synaptic contacts involving ascending processes from γACs, provides a new, likely corruptive node in OPL lateral inhibition networks. At a minimum, this creates a new corrupted network that could likely diminish the center surround opponency critical for precise visual function. This will likely manifest clinically with diminished visual performance prior to the widespread neuronal loss characteristic of late-stage retinal degeneration (Jones et al., 2003; Pfeiffer et al., 2020b). It is also possible, depending on neuron and neurite physiology, that these processes now provide a novel feedback loop between the IPL and OPL. These results identify the neurons involved in early neurite outgrowth and defines which cells are postsynaptic partners to these aberrant processes, leading to further questions about cell to cell recognition in plasticity and

how it can might be controlled experimentally and therapeutically. In the future, computational modeling of these altered networks is necessary to provide greater insight into the effects of these network changes on visual processing.

5. Pathoconnectomes provide a map for therapeutics

In conclusion, this study introduces the first ultrastructural pathoconnectome and demonstrates the applicability of pathoconnectomics for understanding rewiring in progressive retinal degenerative disease. Retinal remodeling exhibits the same components as CNS negative plasticity in disease, as well as similar proteomic findings observed in neurodegenerative diseases like Alzheimer's, Parkinson's and others (Pfeiffer et al., 2020b). Therefore, beyond its direct applicability to retinal disease, we believe information provided by pathoconnectomics is likely to demonstrate fundamental rules in how neural networks are altered, that are applicable to disorders of the CNS as synaptic partners degenerate. These mechanisms of network changes, including those yet to be seen in pathoconnectomes of more advanced degeneration, will inform us about the progression, what ultimately causes networks to fail, and describe future targets for therapeutic intervention based on key principles of network plasticity.

Acknowledgements

This work was supported by the National Institutes of Health [RO1 EY015128(BWJ), RO1 EY028927(BWJ), P30 EY014800(Core), T32 EY024234(RLP)]; and an Unrestricted Research Grant from Research to Prevent Blindness, New York, NY to the Department of Ophthalmology & Visual Sciences, University of Utah.

Appendix A. Supplementary data

Supplementary data to this article can be found online at https://doi.org/10.1016/j.exer.2020.108196.

References

Adly, M.A., Spiwoks-Becker, I., Vollrath, L., 1999. Ultrastructural changes of photoreceptor synaptic ribbons in relation to time of day and illumination. Invest. Ophthalmol. Vis. Sci. 40 (10), 2165–2172.
Agosta, F., Rocca, M.A., Pagani, E., Absinta, M., Magnani, G., Marcone, A., Falautano, M., Comi, G., Gorno-Tempini, M.L., Filippi, M., 2010. Sensorimotor network rewiring in mild cognitive impairment and alzheimer's disease. Hum. Brain Mapp. 31 (4), 515–525.
Anderson, J.R., Jones, B.W., Watt, C.B., Shaw, M.V., Yang, J.H., Demill, D., Lauritzen, J. S., Lin, Y., Rapp, K.D., Mastronarde, D., Koshevoy, P., Grimm, B., Tasdizen, T., Whitaker, R., Marc, R.E., 2011a. Exploring the retinal connectome. Mol. Vis. 17, 355–379.
Anderson, J.R., Jones, B.W., Yang, J.H., Shaw, M.V., Watt, C.B., Koshevoy, P., Spaltenstein, J., Jurrus, E., U, V.K., Whitaker, R.T., Mastronarde, D., Tasdizen, T., Marc, R.E., 2009. A computational framework for ultrastructural mapping of neural circuitry. PLoS Biol. 7 (3), e1000074.
Anderson, J.R., Mohammed, S., Grimm, B., Jones, B.W., Koshevoy, P., Tasdizen, T., Whitaker, R., Marc, R.E., 2011b. The viking viewer for connectomics: scalable multi-user annotation and summarization of large volume data sets. J Microsc 241 (1), 13–28.
Bargmann, C.I., Hartwieg, E., Horvitz, H.R., 1993. Odorant-selective genes and neurons mediate olfaction in c. Elegans. Cell 74 (3), 515–527.
Behrens, C., Schubert, T., Haverkamp, S., Euler, T., Berens, P., 2016. Connectivity map of bipolar cells and photoreceptors in the mouse retina. Elife 5.
Beier, C., Hovhannisyan, A., Weiser, S., Kung, J., Lee, S., Lee, D.Y., Huie, P., Dalal, R., Palanker, D., Sher, A., 2017. Deafferented adult rod bipolar cells create new synapses with photoreceptors to restore vision. J. Neurosci. 37 (17), 4635–4644.
Buck, S., 2004. Rod-cone interactions in human vision. In: Chalupa, L.M., Werner, J. (Eds.), Book Rod-Cone Interactions in Human Vision. MIT Press, Cambridge, MA, pp. 863–878.
Buck, S., 2014. The interaction of rod and cone signals: pathways and psychophysics. In: Werner, J., Chalupa, L.M. (Eds.), Book the Interaction of Rod and Cone Signals: Pathways and Psychophysics. MIT press, Cambridge, MA, pp. 485–497.
Catela, C., Shin, M.M., Dasen, J.S., 2015. Assembly and function of spinal circuits for motor control. Annu. Rev. Cell Dev. Biol. 31, 669–698.
Chew, Y.L., Walker, D.S., Towlson, E.K., Vertes, P.E., Yan, G., Barabasi, A.L., Schafer, W. R., 2017. Recordings of caenorhabditis elegans locomotor behaviour following targeted ablation of single motorneurons. Sci Data 4, 170156.
Creel, D.J., 2019. Electroretinograms. Handb. Clin. Neurol. 160, 481–493.
Day, M., Wang, Z., Ding, J., An, X., Ingham, C.A., Shering, A.F., Wokosin, D., Ilijic, E., Sun, Z., Sampson, A.R., Mugnaini, E., Deutch, A.Y., Sesack, S.R., Arbuthnott, G.W., Surmeier, D.J., 2006. Selective elimination of glutamatergic synapses on striatopallidal neurons in Parkinson disease models. Nat. Neurosci. 9 (2), 251–259.
Dedek, K., Breuninger, T., de Sevilla Muller, L.P., Maxeiner, S., Schultz, K., Janssen-Bienhold, U., Willecke, K., Euler, T., Weiler, R., 2009. A novel type of interplexiform amacrine cell in the mouse retina. Eur J Neurosci 30 (2), 217–228.
delEtoile, J., Adeli, H., 2017. Graph theory and brain connectivity in alzheimer's disease. Neuroscientist 23 (6), 616–626.
Diamond, J.S., 2017. Inhibitory interneurons in the retina: types, circuitry, and function. Annu Rev Vis Sci 3, 1–24.
Dowling, J.E., Ehinger, B., 1975. Synaptic organization of the amine-containing interplexiform cells of the goldfish and cebus monkey retinas. Science 188 (4185), 270–273.
Fariss, R.N., Li, Z.Y., Milam, A.H., 2000. Abnormalities in rod photoreceptors, amacrine cells, and horizontal cells in human retinas with retinitis pigmentosa. Am. J. Ophthalmol. 129 (2), 215–223.
Fei, Y., 2002. Cone neurite sprouting: an early onset abnormality of the cone photoreceptors in the retinal degeneration mouse. Mol. Vis. 8, 306–314.
Fisher, S.K., Lewis, G.P., Linberg, K.A., Barawid, E., Verardo, M.R., 1995. Cellular remodeling in mammalian retina induced by retinal detachment. In: Kolb, H., Fernandez, E., Nelson, R. (Eds.), Book Cellular Remodeling in Mammalian Retina Induced by Retinal Detachment. Salt Lake City (UT).
Fisher, S.K., Lewis, G.P., Linberg, K.A., Verardo, M.R., 2005. Cellular remodeling in mammalian retina: results from studies of experimental retinal detachment. Prog. Retin. Eye Res. 24 (3), 395–431.
Guo, L., Xiong, H., Kim, J.I., Wu, Y.W., Lalchandani, R.R., Cui, Y., Shu, Y., Xu, T., Ding, J. B., 2015. Dynamic rewiring of neural circuits in the motor cortex in mouse models of Parkinson's disease. Nat. Neurosci. 18 (9), 1299–1309.
Hackam, A.S., Strom, R., Liu, D., Qian, J., Wang, C., Ottesen, D., Gunatilaka, T., Farkas, R.H., Chowers, I., Kageyama, M., Leveillard, T., Sahel, J.A., Campochiaro, P. A., Parmigiani, G., Zack, D.J., 2004. Identification of gene expression changes associated with the progression of retinal degeneration in the rd1 mouse. Invest Ophthalmol Vis Sci 45 (9), 2929–2942.
Hamel, C., 2006. Retinitis pigmentosa. Orphanet J. Rare Dis. 1, 40.
Hartong, D.T., Berson, E.L., Dryja, T.P., 2006. Retinitis pigmentosa. Lancet 368 (9549), 1795–1809.
Johnson, R.E., Tien, N.W., Shen, N., Pearson, J.T., Soto, F., Kerschensteiner, D., 2017. Homeostatic plasticity shapes the visual system's first synapse. Nat. Commun. 8 (1), 1220.
Jones, B.W., Kondo, M., Terasaki, H., Lin, Y., McCall, M., Marc, R.E., 2012. Retinal remodeling. Jpn. J. Ophthalmol. 56 (4), 289–306.
Jones, B.W., Kondo, M., Terasaki, H., Watt, C.B., Rapp, K., Anderson, J., Lin, Y., Shaw, M. V., Yang, J.H., Marc, R.E., 2011. Retinal remodeling in the tg p347l rabbit, a large-eye model of retinal degeneration. J. Comp. Neurol. 519 (14), 2713–2733.
Jones, B.W., Marc, R.E., 2005. Retinal remodeling during retinal degeneration. Exp. Eye Res. 81 (2), 123–137.
Jones, B.W., Pfeiffer, R.L., Ferrell, W.D., Watt, C.B., Marmor, M., Marc, R.E., 2016a. Retinal remodeling in human retinitis pigmentosa. Exp. Eye Res. 150, 149–165.
Jones, B.W., Pfeiffer, R.L., Ferrell, W.D., Watt, C.B., Tucker, J., Marc, R.E., 2016b. Retinal remodeling and metabolic alterations in human amd. Front. Cell. Neurosci. 10, 103.
Jones, B.W., Watt, C.B., Frederick, J.M., Baehr, W., Chen, C.K., Levine, E.M., Milam, A. H., Lavail, M.M., Marc, R.E., 2003. Retinal remodeling triggered by photoreceptor degenerations. J. Comp. Neurol. 464 (1), 1–16.
Kalloniatis, M., Fletcher, E.L., 2004. Retinitis pigmentosa: understanding the clinical presentation, mechanisms and treatment options. Clin. Exp. Optom. 87 (2), 65–80.
Kalloniatis, M., Marc, R.E, 1990. Interplexiform cells of the goldfish retina. J Comp Neurol 297 (3), 340–358.
Kolb, H., Famiglietti, E.V., 1974. Rod and cone pathways in the inner plexiform layer of cat retina. Science 186 (4158), 47–49.
Kondo, M., Sakai, T., Komeima, K., Kurimoto, Y., Ueno, S., Nishizawa, Y., Usukura, J., Fujikado, T., Tano, Y., Terasaki, H., 2009. Generation of a transgenic rabbit model of retinal degeneration. Invest. Ophthalmol. Vis. Sci. 50 (3), 1371–1377.
Lacor, P.N., Buniel, M.C., Furlow, P.W., Clemente, A.S., Velasco, P.T., Wood, M., Viola, K. L., Klein, W.L., 2007. Abeta oligomer-induced aberrations in synapse composition, shape, and density provide a molecular basis for loss of connectivity in alzheimer's disease. J. Neurosci. 27 (4), 796–807.
Lauritzen, J.S., Anderson, J.R., Jones, B.W., Watt, C.B., Mohammed, S., Hoang, J.V., Marc, R.E., 2013. On cone bipolar cell axonal synapses in the off inner plexiform layer of the rabbit retina. J. Comp. Neurol. 521 (5), 977–1000.
Lauritzen, J.S., Sigulinsky, C.L., Anderson, J.R., Kalloniatis, M., Nelson, N.T., Emrich, D. P., Rapp, C., McCarthy, N., Kerzner, E., Meyer, M., Jones, B.W., Marc, R.E., 2019. Rod-cone crossover connectome of mammalian bipolar cells. J. Comp. Neurol. 527 (1), 87–116.
Lee, W.C., Bonin, V., Reed, M., Graham, B.J., Hood, G., Glattfelder, K., Reid, R.C., 2016. Anatomy and function of an excitatory network in the visual cortex. Nature 532 (7599), 370–374.
Lewis, G.P., Linberg, K.A., Fisher, S.K., 1998. Neurite outgrowth from bipolar and horizontal cells after experimental retinal detachment. Invest. Ophthalmol. Vis. Sci. 39 (2), 424–434.

Lin, Y., Jones, B.W., Liu, A., Tucker, J.F., Rapp, K., Luo, L., Baehr, W., Bernstein, P.S., Watt, C.B., Yang, J.H., Shaw, M.V., Marc, R.E., 2012. Retinoid receptors trigger neuritogenesis in retinal degenerations. Faseb. J. 26 (1), 81–92.
Lin, B., Masland, R.H., Strettoi, E., 2009. Remodeling of cone photoreceptor cells after rod degeneration in rd mice. Experimental Eye Research 88 (3), 589–599.
Linberg, K.A., Lewis, G.P., Matsumoto, B., Fisher, S.K., 2006. Immunocytochemical evidence that rod-connected horizontal cell axon terminals remodel in response to experimental retinal detachment in the cat. Mol. Vis. 12, 1674–1686.
Lujan, B.J., Roorda, A., Croskrey, J.A., Dubis, A.M., Cooper, R.F., Bayabo, J.K., Duncan, J.L., Antony, B.J., Carroll, J., 2015. Directional optical coherence tomography provides accurate outer nuclear layer and henle fiber layer measurements. Retina 35 (8), 1511–1520.
Marc, R.E., 2010. Injury and repair: retinal remodeling. In: Dartt, D. (Ed.), Book Injury and Repair: Retinal Remodeling. Elsevier, pp. 414–420.
Marc, R.E., Anderson, J.R., Jones, B.W., Sigulinsky, C.L., Lauritzen, J.S., 2014. The aii amacrine cell connectome: a dense network hub. Front. Neural Circ. 8, 104.
Marc, R.E., Cameron, D., 2002. A molecular phenotype atlas of the zebrafish retina. J. Neurocytol. 30 (7), 593–654.
Marc, R.E., Jones, B.W., 2002. Molecular phenotyping of retinal ganglion cells. The Journal of Neuroscience 22 (2), 413–427.
Marc, R.E., Jones, B.W., Anderson, J.R., Kinard, K., Marshak, D.W., Wilson, J.H., Wensel, T., Lucas, R.J., 2007. Neural reprogramming in retinal degeneration. Invest. Ophthalmol. Vis. Sci. 48 (7), 3364–3371.
Marc, R.E., Jones, B.W., Lauritzen, J.S., Watt, C.B., Anderson, J.R., 2012. Building retinal connectomes. Curr. Opin. Neurobiol. 22 (4), 568–574.
Marc, R.E., Jones, B.W., Watt, C.B., Anderson, J.R., Sigulinsky, C., Lauritzen, S., 2013. Retinal connectomics: towards complete, accurate networks. Prog. Retin. Eye Res. 37, 141–162.
Marc, R.E., Jones, B.W., Watt, C.B., Strettoi, E., 2003. Neural remodeling in retinal degeneration. Prog. Retin. Eye Res. 22 (5), 607–655.
Marc, R.E., Murry, R.F., Basinger, S.F., 1995. Pattern recognition of amino acid signatures in retinal neurons. J. Neurosci. 15 (7 Pt 2), 5106–5129.
Marc, R.E., Sigulinsky, C.L., Pfeiffer, R.L., Emrich, D., Anderson, J.R., Jones, B.W., 2018. Heterocellular coupling between amacrine cells and ganglion cells. Front. Neural Circ. 12, 90.
Masland, R.H., 2012. The neuronal organization of the retina. Neuron 76 (2), 266–280.
Morimoto, K., Fahnestock, M., Racine, R.J., 2004. Kindling and status epilepticus models of epilepsy: rewiring the brain. Prog Neurobiol 73 (1), 1–60.
O'Brien, J., Nguyen, H.B., Mills, S.L., 2004. Cone photoreceptors in bass retina use two connexins to mediate electrical coupling. J Neurosci 24 (24), 5632–5642.
Ottersen, O.P., 1989. Quantitative electron microscopic immunocytochemistry of neuroactive amino acids. Anat. Embryol. 180 (1), 1–15.
Oyster, C.W., Takahashi, E.S., 1977. Interplexiform cells in rabbit retina. Proc R Soc Lond B Biol Sci 197 (1129), 477–484.
Pang, J.J., Yang, Z., Jacoby, R.A., Wu, S.M., 2018. Cone synapses in mammalian retinal rod bipolar cells. J. Comp. Neurol. 526 (12), 1896–1909.
Peng, Y.W., Hao, Y., Petters, R.M., Wong, F., 2000. Ectopic synaptogenesis in the mammalian retina caused by rod photoreceptor-specific mutations. Nat. Neurosci. 3 (11), 1121–1127.
Pfeiffer, R.L., Anderson, J.R., Emrich, D.P., Dahal, J., Sigulinsky, C.L., Morrison, H.A.B., Yang, J.H., Watt, C.B., Rapp, K.D., Kondo, M., Terasaki, H., Garcia, J.C., Marc, R.E., Jones, B.W., 2019. Pathoconnectome analysis of muller cells in early retinal remodeling. Adv. Exp. Med. Biol. 1185, 365–370.
Pfeiffer, R.L., Marc, R.E., Jones, B.W., 2020a. Muller cell metabolic signatures: evolutionary conservation and disruption in disease. Trends Endocrinol Metab 31 (4), 320–329.
Pfeiffer, R.L., Marc, R.E., Jones, B.W., 2020b. Persistent remodeling and neurodegeneration in late-stage retinal degeneration. Prog. Retin. Eye Res. 74, 100771.
Samuel, M.A., Zhang, Y., Meister, M., Sanes, J.R., 2011. Age-related alterations in neurons of the mouse retina. J. Neurosci. 31 (44), 16033–16044.
Schmid, L.C., Mittag, M., Poll, S., Steffen, J., Wagner, J., Geis, H.R., Schwarz, I., Schmidt, B., Schwarz, M.K., Remy, S., Fuhrmann, M., 2016. Dysfunction of somatostatin-positive interneurons associated with memory deficits in an alzheimer's disease model. Neuron 92 (1), 114–125.
Schmitz, F., 2014. Presynaptic [ca(2+)] and gcaps: aspects on the structure and function of photoreceptor ribbon synapses. Front. Mol. Neurosci. 7, 3.
Shen, N., Wang, B., Soto, F., Kerschensteiner, D., 2020. Homeostatic plasticity shapes the retinal response to photoreceptor degeneration. Curr. Biol. 30 (10), 1916–1926.
Sigulinsky, C.L., Anderson, J.R., Kerzner, E., Rapp, C.N., Pfeiffer, R.L., Rodman, T.M., Emrich, D.P., Rapp, K.D., Nelson, N.T., Lauritzen, J.S., Meyer, M., Marc, R.E., Jones, B.W., 2020. Network architecture of gap junctional coupling among parallel processing channels in the mammalian retina. J. Neurosci. 40 (23), 4483–4511.
Spiwoks-Becker, I., Glas, M., Lasarzik, I., Vollrath, L., 2004. Mouse photoreceptor synaptic ribbons lose and regain material in response to illumination changes. Eur. J. Neurosci. 19 (6), 1559–1571.
Stabell, B., Stabell, U., 2002. Effects of rod activity on color perception with light adaptation. J Opt Soc Am A Opt Image Sci Vis 19 (7), 1249–1258.
Stefanov, A, Novelli, E, Strettoi, E, 2020. Inner retinal preservation in the photoinducible i307n rhodopsin mutant mouse, a model of autosomal dominant retinitis pigmentosa. J Comp Neurol 528 (9), 11020–11025.
Strettoi, E., Pignatelli, V., 2000. Modifications of retinal neurons in a mouse model of retinitis pigmentosa. Proc. Natl. Acad. Sci. U. S. A. 97 (20), 11020–11025.
Strettoi, E., Porciatti, V., Falsini, B., Pignatelli, V., Rossi, C., 2002. Morphological and functional abnormalities in the inner retina of the rd/rd mouse. J. Neurosci. 22 (13), 5492–5504.
Thoreson, W.B., Dacey, D.M., 2019. Diverse cell types, circuits, and mechanisms for color vision in the vertebrate retina. Physiol. Rev. 99 (3), 1527–1573.
Thoreson, W.B., Witkovsky, P., 1999. Glutamate receptors and circuits in the vertebrate retina. Prog. Retin. Eye Res. 18 (6), 765–810.
Tien, N.W., Soto, F., Kerschensteiner, D., 2017. Homeostatic plasticity shapes cell-type-specific wiring in the retina. Neuron 94 (3), 656–665 e4.
Tsukamoto, Y., Omi, N., 2013. Functional allocation of synaptic contacts in microcircuits from rods via rod bipolar to aii amacrine cells in the mouse retina. J. Comp. Neurol. 521 (15), 3541–3555.
Tsukamoto, Y., Omi, N., 2014. Some off bipolar cell types make contact with both rods and cones in macaque and mouse retinas. Front. Neuroanat. 8, 105.
Tsukamoto, Y., Omi, N., 2015. Off bipolar cells in macaque retina: type-specific connectivity in the outer and inner synaptic layers. Front. Neuroanat. 9, 122.
Ueno, S., Kominami, T., Okado, S., Inooka, D., Kondo, M., Terasaki, H., 2019. Course of loss of photoreceptor function and progressive muller cell gliosis in rhodopsin p347l transgenic rabbits. Exp. Eye Res. 184, 192–200.
White, J.G., Southgate, E., Thomson, J.N., Brenner, S., 1986. The structure of the nervous system of the nematode caenorhabditis elegans. Philos. Trans. R. Soc. Lond. B Biol. Sci. 314 (1165), 1–340.